Applying Ampere's Law Integral to Ørsted and CHAMP Overflights

Rob Shore[1],Susan Macmillan[2] , Kathy Whaler[1], Ciaran Beggan[2]
Authors' affiliation: [1]: University of Edinburgh, [2]: British Geological Survey
Contact email of first author: R.M.Shore@sms.ed.ac.uk

We seek to characterise and quantify current flow in the high-altitude ionosphere. The Ampère's law integral is applied to the closed loop formed by the radial arc of the overflight of the CHAMP and Ørsted magnetic satellites. Throughout the period 2000-2005, we solve for ionospheric current flow in the region between the two satellites at discrete intervals and a range of local times.

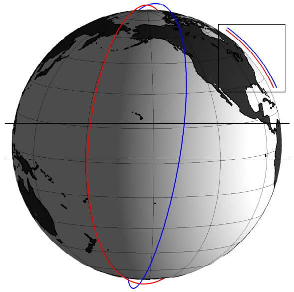

Figure 1: Single orbit of **CHAMP** and **Ørsted** data, with a single overlap region shown as a pair of arcs

For each epoch of coinciding local time (Fig 9), overlapping arcs of length 25 degrees colatitude are selected (Fig 1). The Ampère's law integral is applied to the magnetic data of these arcs, solving for current flow in the region between the overflights (refer to schematic in Figure 2). Integral direction is held consistent for each overlap instance, and solution magnitudes are normalised by the surface area of the enclosure, providing values for current density (process flow in Fig 3).

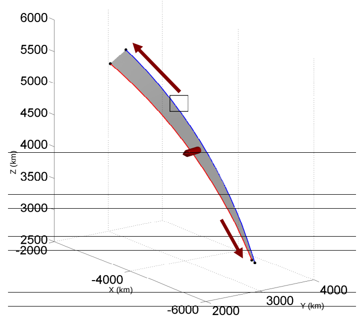

Figure 2: Solution area geometry in Cartesian coordinates (wrt Earth's centre). Integral setup: red arrows indicate integral direction, red cone-vector indicates direction of resolution of current flow through arcs. The integral loop is formed by the two arcs and is closed fictitiously across the radial gaps.

$$\oint B \cdot dl = \mu_0 I$$

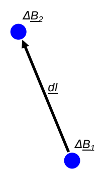

Stages in calculation:

- Vector magnetic data ($\underline{B}$)
  - remove main field estimate ($\underline{B} - \underline{B}_{MF} = \Delta\underline{B}$)
- Main-field-removed vector data ($\Delta\underline{B}$)
  - take difference of points ($\Delta\underline{B}_2 - \Delta\underline{B}_1$)
- $\underline{dB}$ for two successive measurement points
  - take dot product ($\underline{dB} \cdot \underline{dl}$)
- nT.km contribution value for 8km line element
  - (sum of contributions for circumference)/μ_0
- Current flow in μA for calculation area
  - divide by integral circuit surface area
- Solution for current flow through region in A/m²

Figure 3: Arc integral application: single line element, Ørsted data

The upper F region of the ionosphere lies between the Ørsted and CHAMP orbits. Current flow here is less linked to insolation than in the lower-altitude E region ionosphere, and is instead driven by the Earth's gravity field, and pressure differences in the ionosphere. The effects of these currents at CHAMP altitude (350-450 km) are well documented. We assess their impact between Ørsted and CHAMP altitudes, with a view to developing a processing tool for constellation missions.

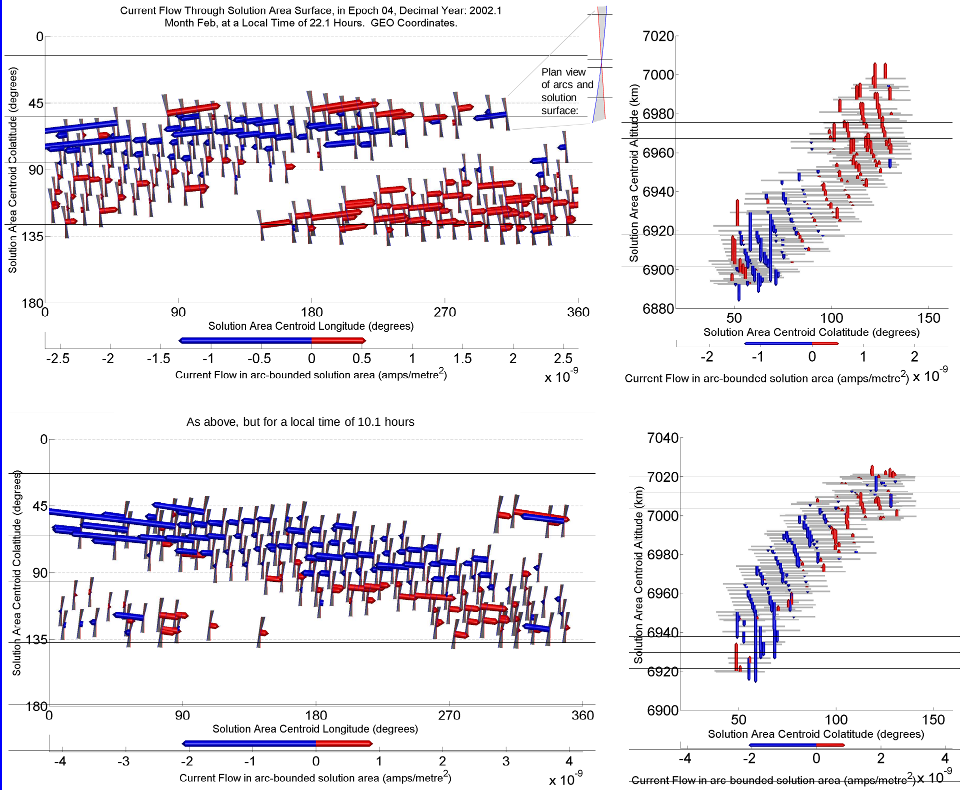

Figure 10: Solutions for current density in the two local time overlaps in February 2002. Vectors stem from the centroid of the area surface and are colour-coded by sign. For each local time, two aspects of the same data are plotted: longitude versus latitude, and latitude versus altitude. Solutions show good local agreement within separate hemispheres, and the method appears to break down as the poles are approached.

The magnetospheric field has a significant effect on the solutions, but we have not applied a correction for this indiscriminately: here we assess the solutions with and without using CM4 to correct for magnetospheric and crustal fields. Data density between epochs varies: here we show the uncorrected solution spread for an epoch of high data density (Fig 10), and the effect of applying the CM4 correction on an epoch of low data density (Fig 11). The results show that CM4 improves the estimate, but gravity currents are effectively resolved in quiet periods even without the correction. Altitude variance is also a concern: signals at a range of altitudes are easily obtained, but less easily filtered to an unbiased characteristic signal.

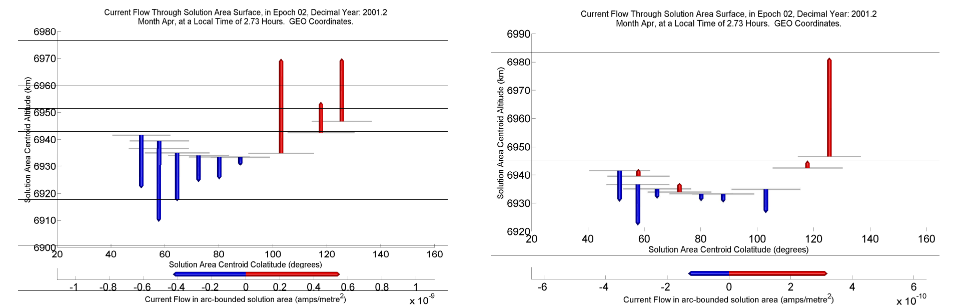

Figure 11: Solutions for current density in a single local time overlap in April 2001. The figure on the left shows the solutions without the CM4 correction for magnetospheric and crustal fields, whilst the figure on the right shows the same solutions, but with the CM4 correction applied.

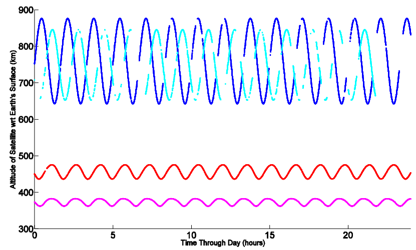

Figure 8: Altitude progression of the two satellites: Blue, Red: Ørsted and CHAMP near mission start, Cyan, Magenta: Ørsted, CHAMP near start of 2005.

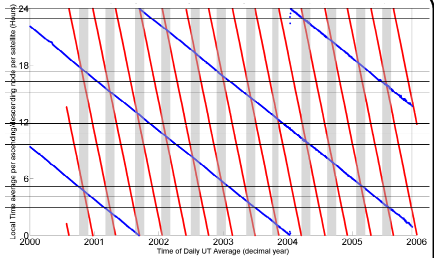

Figure 9: Epochs of Local Time overlap of **CHAMP** and **Ørsted** ascending and descending nodes (areas of ±2 hours local time about each overlap are shaded).

The altitude variance in a single day of Ørsted data is greater than the altitude decay of CHAMP through 2000 to 2005. Altitude effects are therefore resolvable, but not in a controlled manner. Dual-aspect plots of the vector maps have been used to highlight this. Note that the maps of vector solutions span 5 days each, but all arcs are within half an hour of each other.

Ritter, P. & Lühr, H., 2006. Curl-B technique applied to Swarm constellation for determining field-aligned currents, *Earth Planets and Space*, 58, 463-476.

Stauning, P. & Primdahl, F., 2000. First detection of global dawn-dusk ionospheric current intensities using Ampère's integral law on Ørsted orbits, *Geophys. Res. Lett.*, 27, 3273-3276.

Maus, S. & Luhr, H., 2006. A gravity-driven electric current in the Earth's ionosphere identified in CHAMP satellite magnetic measurements, *Geophys. Res. Lett.*, 33, 5.

The integrals are closed fictitiously across the radial gap between the arcs' edge-points – we assume that these contributions can be neglected. This will be more true for longer arcs, but these risk over-smoothing our data. Here we show the results of testing the error inherent in the arc setup throughout a large range of arc lengths – each test showed increased solution stability and accuracy at the chosen arc length of 25 degrees colatitude.

We test the error from neglecting radial closure by predicting the magnetic field from an input current (aligned with the area surface normal) onto the arcs' data positions. We solve for current flow from this forward modelled data and compare the input and recovered models. Figure 4 shows the percentage recovery for these tests.

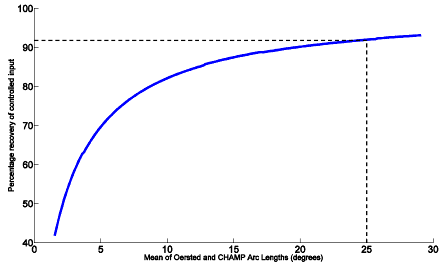

Figure 4: Percentage recovery from inverting a controlled-input forward model.

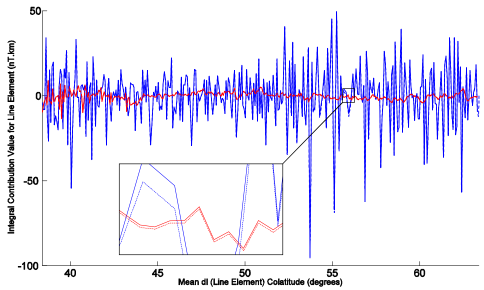

Figure 5: Along-arc variance in each line element integral contribution value. Effect of CM4 correction shown as a dashed line. Ørsted: blue, CHAMP: red. Each arc is 6 minutes long.

The Ørsted line-element integral contributions are much more variant than those of CHAMP (Fig 5, showing a single arc segment). Applying CM4 to correct for magnetospheric fields has a minimal effect on this variance (though it has a significant effect on the resultant solution). Since we cannot correct for the variance, we have tailored the arc geometry to screen it out. Figures 6 and 7 show that arc lengths of 25 degrees (and greater) offer increased solution stability. The smoothing associated with arcs of this length is not expected to impinge upon the required spatial or temporal resolution for typical current flow at these altitudes.

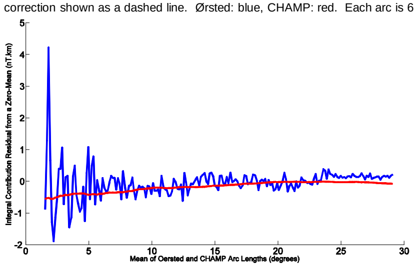

Figure 6: Mean of Ørsted (blue) and CHAMP (red) along-arc integral contribution values: the deviation from a zero mean shows how the high Ørsted variance levels off as more points effectively damp its effect.

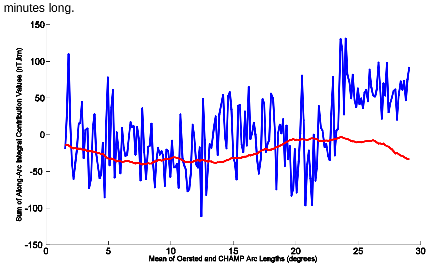

Figure 7: Sum of Ørsted (blue) and CHAMP (red) along-arc integral contribution values: shows how the arc's solution value changes with increasing arc length – increased stability from 25 degrees onwards.